*Classified Seminar on Applications of Electromagnetic Launch Technology*
*Washington, DC, 2–4 May 2007*

# Energy Storage Generator Thermal Analysis for An Electromagnetic Aircraft Launch System

**H-P. Liu, R. D. Lenhart, M. C. Lewis, M. D. Werst, and R. C. Zowarka**

**Center for Electromechanics**
**The University of Texas at Austin**
**1 University Station, R7000**
**Austin, TX 78712**

Abstract—This paper presents thermal analysis predictions of a main generator, which is a primary part of an energy storage subsystem of an electromagnetic aircraft launch system. Three-dimensional finite element thermal models for both main generator rotor and stator have been developed and transient thermal analyses have been performed for various aircraft launching duty cycles. Generator conductors and various insulations are smeared and equivalent thermal properties are used in the thermal analyses to reduce modeling and computational effort. Position-dependent and time-dependent air cooling boundary conditions, which include air temperatures and forced convection heat-transfer coefficients, are determined by transient energy balances, air temperatures, and rotating configurations.

## I. INTRODUCTION

Energy storage subsystem (ESS) generators have been designed to provide electrical pulses to launch aircrafts from aircraft carriers under various launching duty cycles. The ESS generator unit is comprised of main generator, charging induction motor, exciter, and cooling air blowers with integral heat exchanger. Heat losses generated in the machines include electrical losses during discharges, windage frictional losses, and bearing and seal losses. These losses need to be removed to prevent generator rotors and stators from overheating.

Typically, thermal limitation of an electric machine is the electrical insulation. For the ESS generators, insulation materials that can be continuously operated at 180°C (Class H insulation) were chosen. To ensure a 50-year service life from the insulation, a cooling system has been designed such that the maximum machine transient temperatures of the ESS electrical components will not exceed 150°C.

Since the generators are discharged intermittently, a simple active rotor/stator air-gap cooling system has been designed to remove the rotor and stator heat losses generated in the main generator, induction motor, exciter, and rotating diodes. The air coolant, pressurized and circulated by external blowers, is introduced from both ends of the machine and directed to flow through end turns and air gaps of various electrical components. The air streams finally merge in the middle section of the machine and exhaust from central radial vents in the main stator and stator housing. The hot air discharged from the generators is ducted to a sea water heat exchanger for heat removal. The cooled air is then pressurized by the air blowers and ducted back to the generators. The airflow paths within the ESS machine are shown graphically in figure 1.

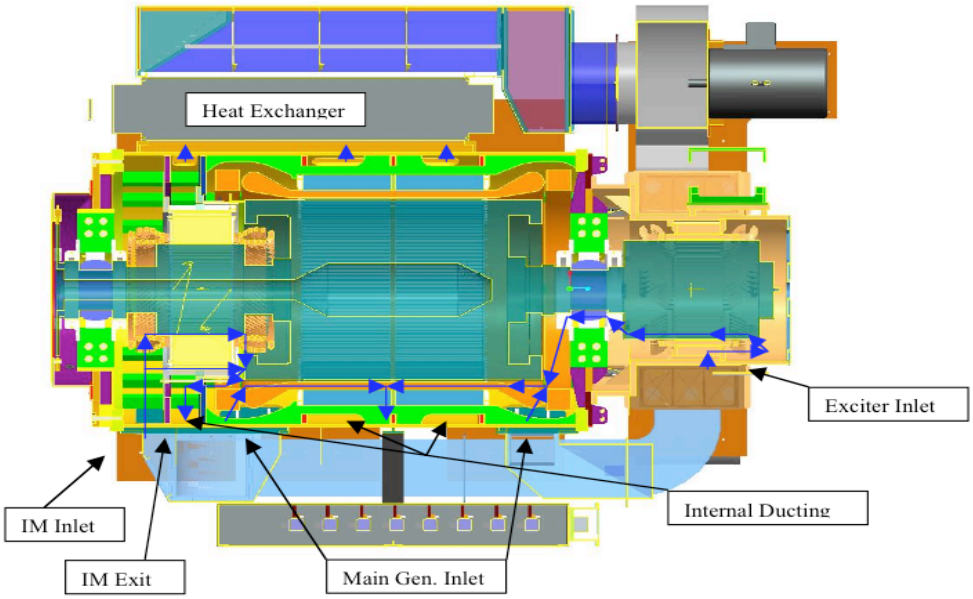


Figure 1. Airflow paths in ESS generator

## II. ESS WINDAGE LOSSES

As compared to electrical and bearing losses, the high energy storage generator windage loss at a rotor peak speed of 4,200 rpm becomes the dominant loss. Frictional windage losses result from a steady and relative motion of two surfaces that are separated by a fluid. In rotating electrical machines which have either non-ventilated or ventilated airflow, the windage losses are generated at those places where relative motions exist between the solid surfaces and the surrounding air. A significant portion of the ESS windage loss occurs in the annular air gap between the main generator rotor and stator due to the high rotor surface velocities and a relatively small radial air gap.

The annular air gap flow between concentric cylinders with a rotating inner cylinder and a stationary outer cylinder is commonly referred as a Couette flow. The flow regimes associated with a wall-driven air-gap air flow are very complicated. For a continuum flow between concentric rotating cylinders, secondary flow of rows of circumferential Taylor vortices in the air gap due to centrifugal flow instability of a curved flow at relatively high rotating speeds will typically be formed. The classical continuum flow of a linear Newtonian viscous fluid, described by the Navier-Stokes momentum equations, assumes the fluid is a continuous medium in which the viscous shear stresses are linearly proportional to the strain rates. The Navier-Stokes shear stress calculation imparts zero-slip flow boundary conditions at the interfaces between the fluid and the solid. For an annular rotating continuum flow, various flow regimes exist, such as laminar, transition, vortex, and turbulent flows. Calculations of continuum flow windage drags on smooth rotating cylinders and disks are mostly carried out by using empirically determined torque coefficients [1].

Smooth rotating surfaces introduce minimum windage friction resistances. To analytically or semi-analytically quantify the roughness effect on the windage loss is extremely challenging. Although computational fluid dynamics (CFD) analysis could be used to analyze the roughness effect; however, the extensive CFD computation effort typically limits it to a local area in the entire machine. The accuracies associated with CFD predictions are unknown unless validated by experimental results. The windage drag depends on the density of the roughness distribution, such as the number of protrusions per unit area, the heights and shapes of the protrusions, and the way in which these protrusions are distributed over the surfaces. Windage test data for rotating concentric cylinders which are physically rough have been reported previously [2], in which an almost one-order of magnitude difference in torque coefficient between the roughest test configuration and the physically smooth cylinders was indicated.

To consider the effect of ESS surface roughness caused by the stacking of rotor and stator laminates on the windage drags, windage tests at various generator speeds have been performed to quantify the windage losses and validate a semi-analytical windage loss prediction model developed by The Center for Electromechanics at The University of Texas at Austin (UT-CEM). The predicted and measured ESS windage and bearing losses are shown in figure 2.

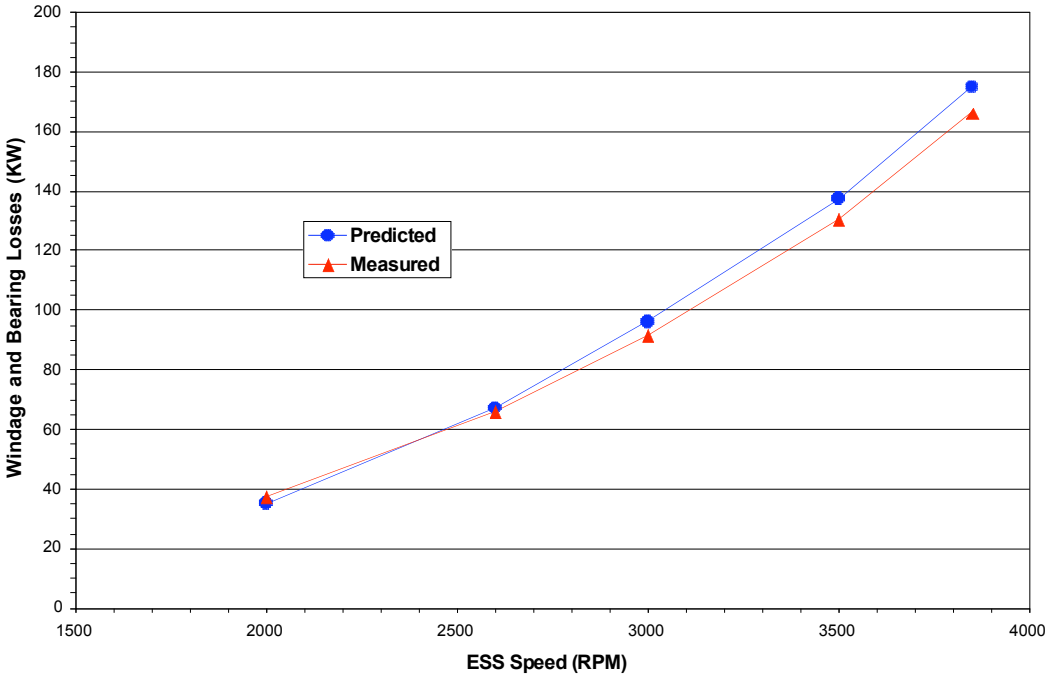


Figure 2. ESS windage and bearing losses

## III. MAIN GENERATOR DESIGN AND LOSSES

The main generator rotor is a 1 x 16 strip wound field coil design with 16 turns of copper conductor in each of the rotor slots. As for the main generator stator design, there are 18 standard-sized copper conductors in each half of the stator slots. Six conductors form a turn; as a result, there are three turns in each half of the stator slots. Two coils are separated by a mid stick in each stator slot. The stator is vacuum impregnated and the dimensional and assembly tolerances are filled with potting resin. The ESS main generator rotor and stator slot details are shown in figures 3 and 4.

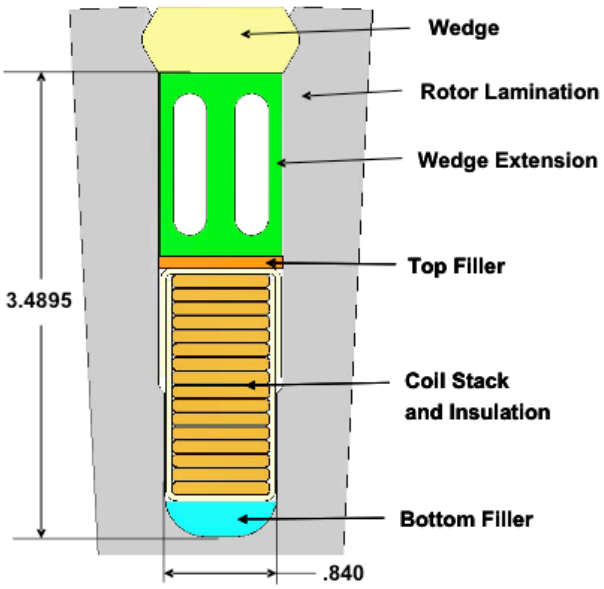


Figure 3. ESS main generator rotor slot detail

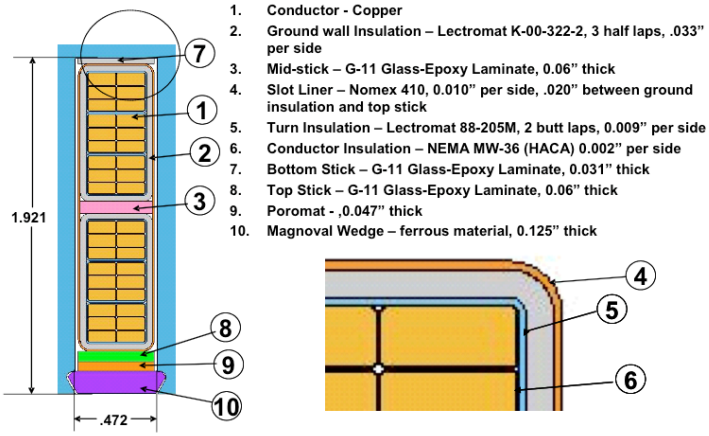


Figure 4. ESS main generator stator slot detail

The aircraft launching duties include carrier qualifications (CQ), cyclic operations, and special operations. This paper only presents 3-D transient main generator thermal analysis for carrier qualifications. The ESS maintains a constant speed of 3,000 rpm during 1-hr standby prior to start of CQ launch sequence. A total of 32 CQ launches are completed in 48 min, which is one launch every 90 s, followed by 12-min ESS idling at 3,000 rpm. The entire CQ launching event consists of 14 of this 1-hr group launches. Table 1 shows the predicted ESS main generator heat losses, in which the main rotor and stator winding dc losses were calculated at an elevated temperature of 150°C and stator slot ac losses were also included. For simplicity, the motoring details from 3,000 rpm to 3,940 rpm prior to the first launch and deceleration from 3,940 RPM to 3,000 rpm between group launches were ignored. Table 2 shows the ESS temperatures used in the thermal analysis.

Table 1. Predicted ESS main generator heat losses during carrier qualifications launches

| Time Period | ESS Speed (RPM) | Rotor Winding (KW) | Rotor Core (KW) | Stator Winding (KW) | Stator Lam. Teeth and Yoke (KW) | Windage (KW) | Total (KW) |
|---|---|---|---|---|---|---|---|
| 0 ® 1 hr (1-hr Standby) | 3000 | 0 | 0 | 0 | 0 | 70.97 | 70.97 |
| 3600 s ® 3687 s (87-s Motoring) | 3940 ® 4200 | 0 | 0 | 0 | 0 | 170.83 | 170.83 |
| 3687 s ® 3690 s (3-s Launching) | 4200 ® 3940 | 21.55 | 84 | 24.92 | 365 | 171.9 | 667.37 |
| 1hr48 min ® 2 hr (12-min Idling) | 3000 | 0 | 0 | 0 | 0 | 70.97 | 70.97 |

Table 2. ESS temperatures used in thermal analysis
(Degree Celsius for temperature values in parentheses)

| Seawater Temp. (°F) | ESS Compartment Air Temp. (°F) | ESS Initial Temp. (°F) | ESS Air Temp. at Heat Exchanger Exit (°F) | Air Temp. Rise by Fan Pressurization (°F) | ESS inlet Air Temp. (°F) |
|---|---|---|---|---|---|
| 85 (29.4) | 105 (40.6) | 105 (40.6) | 110 (43.3) | 13.5 (7.5) | 123.5 (50.8) |

## IV. TRANSIENT 3-D THERMAL MODELING

Since the rotor and stator end-turn cooling could influence the main generator temperatures in the core region, 3-D finite element thermal modeling for both the main generator rotor and stator have been developed and transient 3-D thermal analyses have been performed for CQ aircraft group launching. It is not practical to consider rotor and stator slot conductor and insulation details in transient 3-D thermal models; instead, the slot conductors and various insulations were smeared and equivalent thermal properties were used in the thermal analyses to reduce modeling and computational effort. Due to geometrical symmetries, only sectors of the main generator rotor and stator were actually modeled. The transient thermal modeling has been performed under the following conditions:

- Consider time-dependent heat losses
    1. Initial standby (1 hr)
       : windage loss at 3,000 rpm
    2. CQ discharge/re-motoring cycles for 32 launches (48 min)
       : windage loss (3,940 rpm to 4,200 rpm) and electrical loss (3-s launching only)
    3. Idling between CQ group launches (12 min)
       : windage loss at 3,000 rpm
    4. Repeat (2) and (3) for seven CQ group launches
- Consider time-dependent and position-dependent air cooling boundary conditions by assuming 100% windage and electrical losses removed on a time-averaged basis

- Spread 3-s discharge electrical losses evenly within 90-s discharge/re-motoring
- Cooling airflow rates predicted by ESS airflow network analysis
  - induction motor airflow rate = 5,354 SCFM
  - main rotor/stator radial air gap airflow rate
    = 1,655 SCFM (induction motor end), 2,102 SCFM (exciter end)
- Lump rotor slot conductors/insulations and use smeared properties in rotor slots
- Lump stator slot conductors/insulations and use smeared properties in stator slots
- Main generator initial temperature = 40.6°C (105°F)

A system-level flow network modeling software [3] has been used to perform ESS airflow analysis. The airflow system was represented as a network of components and flow paths. The characteristics of the network components and flow paths were defined according to the generator design. The airflow system was converted into a network of nodes and links. Conservations of mass, momentum, and energy were enforced over these nodes and links. Distributions of airflow rates, air pressures, and airflow velocities in the ESS were predicted from this airflow network analysis.

The generator component losses and air cooling boundary conditions for the transient 3-D rotor and stator thermal analyses are shown in figures 5 and 6. As shown in figure 6, the open space between the stator lamination outer-diameter surface and stator housing inner-diameter surface is the exhaust air duct prior to the ESS air exit. The position and time dependent air temperatures were determined by transient energy balance calculations. The forced convection heat-transfer coefficients are air temperature dependent and rotating configuration dependent [4,5].

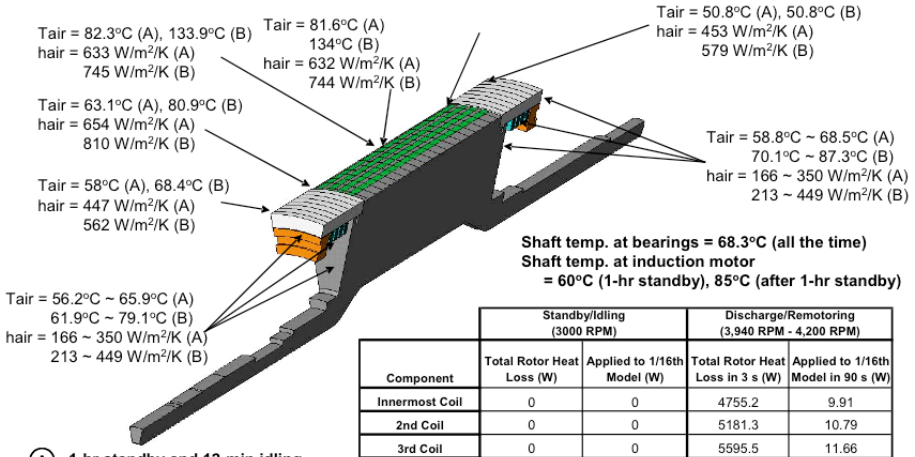


| Component | Standby/Idling (3000 RPM) | | Discharge/Remotoring (3,940 RPM - 4,200 RPM) | |
|---|---|---|---|---|
| | Total Rotor Heat Loss (W) | Applied to 1/16th Model (W) | Total Rotor Heat Loss in 3 s (W) | Applied to 1/16th Model in 90 s (W) |
| Innermost Coil | 0 | 0 | 4755.2 | 9.91 |
| 2nd Coil | 0 | 0 | 5181.3 | 10.79 |
| 3rd Coil | 0 | 0 | 5595.5 | 11.66 |
| Outermost Coil | 0 | 0 | 6018.1 | 12.54 |
| Lamination Teeth | 0 | 0 | 84000 | 175 |

Figure 5. Main generator rotor component heat losses and cooling boundary conditions

| Component | Standby/Idling (3000 RPM) Total Stator Heat Loss (W) | Standby/Idling (3000 RPM) Applied to 1/288th Model (W) | Discharge/Remotoring (3,940 RPM - 4,200 RPM) Total Stator Heat Loss in 3 s (W) | Discharge/Remotoring (3,940 RPM - 4,200 RPM) Applied to 1/288th Model in 90 s (W) |
|---|---|---|---|---|
| Winding in Core Region | 0 | 0 | 16315 | 0.944 (x2) |
| Winding in End-Turn Region | 0 | 0 | 8605 | 0.249 (x4) |
| Stator Lam Teeth and Yoke | 0 | 0 | 365000 | 42.245 |

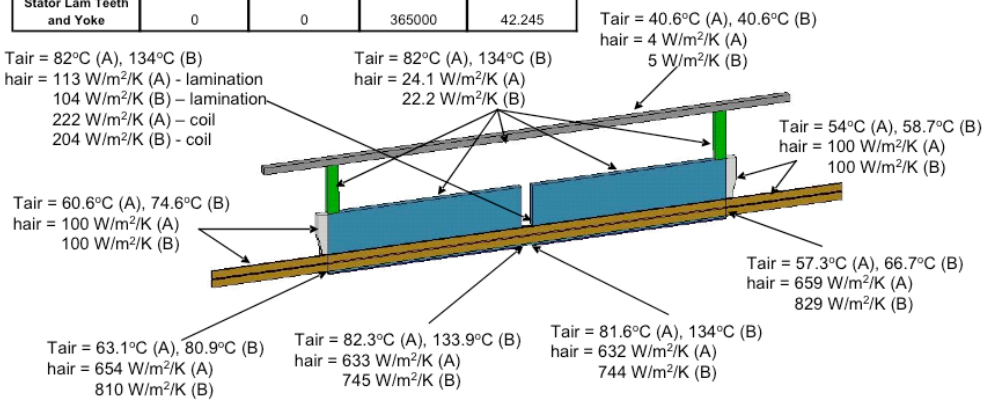


Figure 6. Main generator stator component heat losses and cooling boundary conditions

## V. ESS MAIN GENERATOR THERMAL ANALYSIS RESULTS

The predicted main generator rotor temperature distribution immediately after the seventh CQ launch group (time = 7 hr 48 min) is shown in figure 7. The predicted transient maximum rotor component temperatures are plotted in figure 8. The predicted main generator stator temperature distribution immediately after the seventh CQ launch group (time = 7 hr 48 min) is shown in figure 9. The predicted transient maximum stator component temperatures are plotted in figure 10. The high rotor and stator temperatures, shown in figures 7 and 9, occur at the mid section of the main generator, where the hot air exhausts from the ESS.

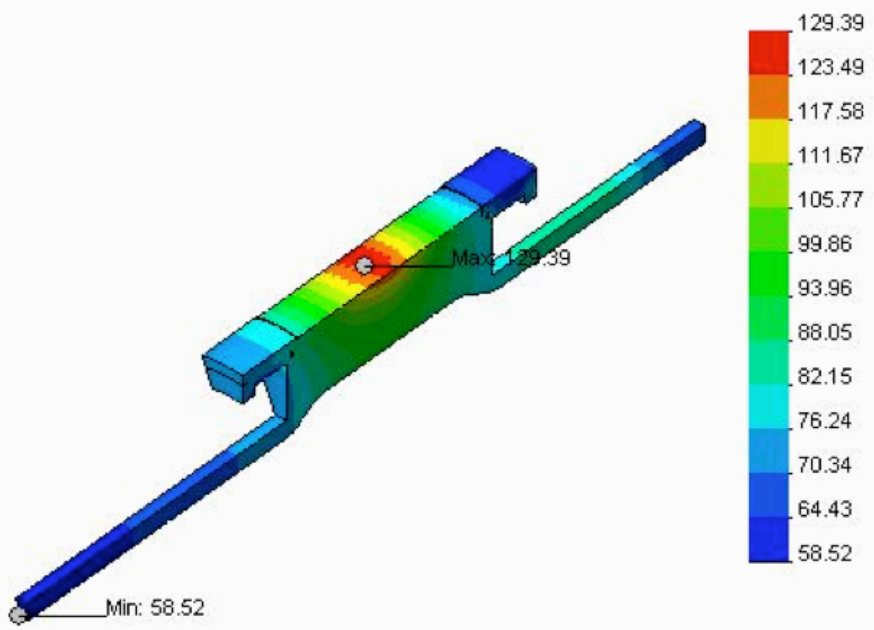


Figure 7. Main generator rotor temperature distribution (°C) immediately after 7th CQ launch group (time = 7 hr 48 min)

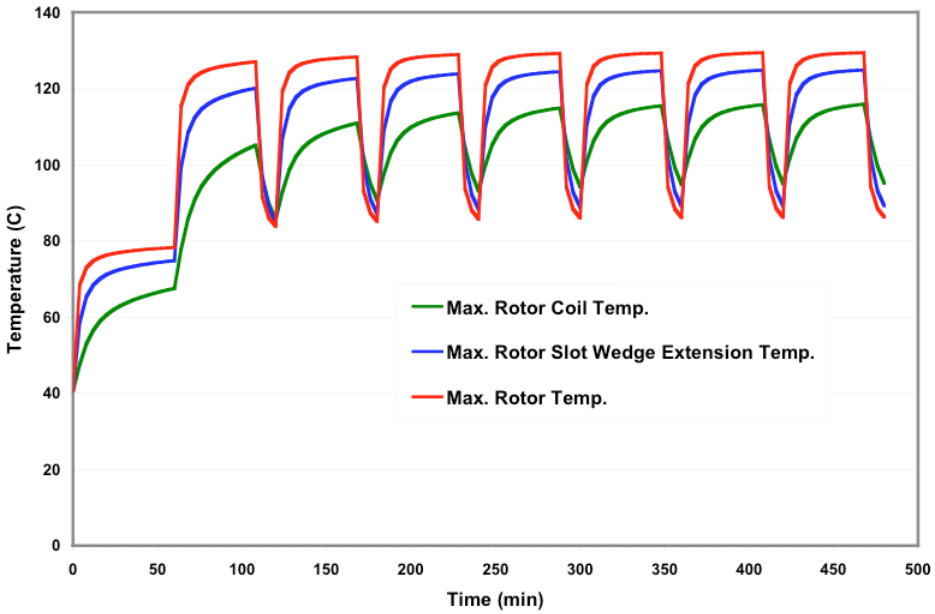


Figure 8. Transient maximum main generator rotor temperatures during CQ duty cycle

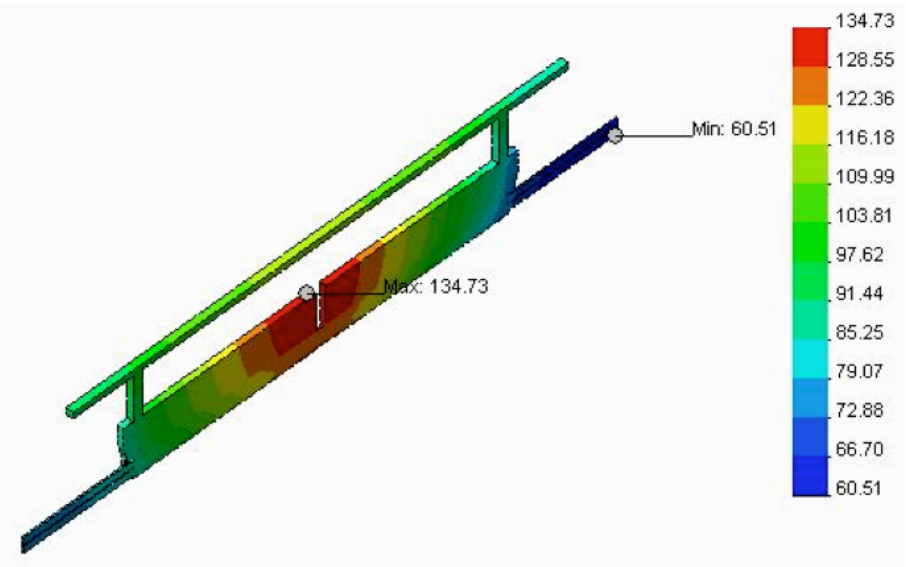


Figure 9. Main generator stator temperature distribution (°C) immediately after 7th CQ launch group (time = 7 hr 48 min)

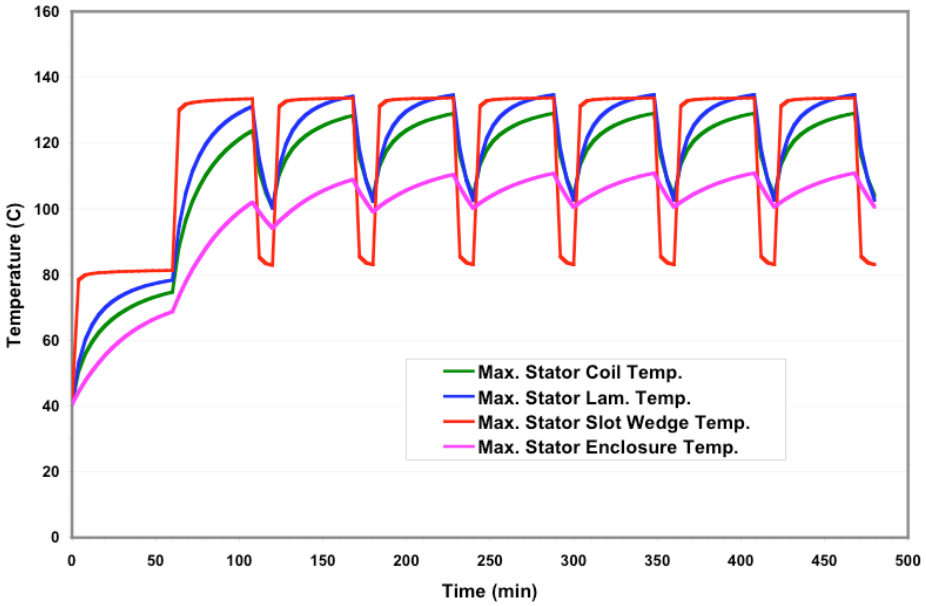


Figure 10. Transient maximum main generator stator temperatures during CQ duty cycle

## VI. CONCLUSIONS

Transient 3-D thermal analyses of an energy storage system generator were performed for a carrier qualifications aircraft launching duty cycle to investigate rotor end-turn cooling, stator end-turn cooling, and axial conduction cooling effect on the rotor and stator temperatures in the core region. Both position and time dependent thermal loads and air cooling boundary conditions are considered in the thermal modeling. It has been found that, on a time-averaged basis, the total windage loss generated in this rotating energy storage system is significantly higher than the total electrical loss produced during the intermittent aircraft launching cycles.

**Acknowledgments**
This research is sponsored by the U.S. Navy through General Atomics under contract number N68335-04-C-0167.

**References**

[1] The General Electric Fluid Flow Data Book, Genium Publishing Corporation, Schenectady, New York, 1994.
[2] D. G. McLaren and H. J. Leutheusser, "Hydrogenerator Windage Loss," General Papers in Fluids Engineering, ASME FED-Vol. 127, 1991.
[3] MacroFlow – A System Modeling and Analysis Tool, Innovative Research, Inc.
[4] C. Gazley, Jr., “Heat-Transfer Characteristics of The Rotational and Axial Flow between Concentric Cylinders,” ASME Transactions, vol. 80, No. 1, pp. 79-90, January 1958.
[5] C. L. Ong, and J. M. Owen, “Computation of The Flow and Heat Transfer due to A Rotating Disc,” International Journal of Heat and Fluid Flow, vol. 12, No. 2, pp. 106-115, June 1991.